NASA CONTRACTOR REPORT

NASA CR-953

INVESTIGATION OF RADIANT HEAT TRANSFER TO PARTICLE-SEEDED GASES FOR APPLICATION TO NUCLEAR ROCKET ENGINE DESIGN

by Edward Y. H. Keng and Clyde Orr, Jr.

Prepared by
GEORGIA INSTITUTE OF TECHNOLOGY
Atlanta, Ga.
for

NATIONAL AERONAUTICS AND SPACE ADMINISTRATION • WASHINGTON, D. C. • NOVEMBER 1967

NASA CR-953

INVESTIGATION OF RADIANT HEAT TRANSFER TO PARTICLE-SEEDED GASES FOR APPLICATION TO NUCLEAR ROCKET ENGINE DESIGN

By Edward Y. H. Keng and Clyde Orr, Jr.

Prepared under Grant No. NsG-273 by
GEORGIA INSTITUTE OF TECHNOLOGY
Atlanta, Ga.

for

NATIONAL AERONAUTICS AND SPACE ADMINISTRATION

For sale by the Clearinghouse for Federal Scientific and Technical Information
Springfield, Virginia 22151 – CFSTI price $3.00

TABLE OF CONTENTS

LIST OF FIGURES

I. SUMMARY

The objective of this research is to provide fundamental information on radiant heat transfer to aerosols to aid in the evaluation of various gaseous-core nuclear rocket concepts. Both theoretical and experimental investigations have been pursued.

View factors have been evaluated for a number of conditions considering a cylindrical geometry for the system, such results being generally applicable to high-temperature technology. The experimental results agree well with theoretical predictions. A new aerosol generator has been designed to produce dense yet uniform aerosols, and preparation for the study of particle evaporation or sublimation in an intense radiant field are underway. An electrically heated tungsten furnace for this investigation is being assembled.

II. INTRODUCTION

Radiant heat transfer is the most important mechanism of transfer at the temperatures involved in gaseous, nuclear, rocket concepts. It is dependent on the opacity characteristics of the propellant gas which may be hydrogen containing small, absorbing particles. Hydrogen gas is practically transparent below $5000^{o}K$[1,2] even under high pressures, thus the radiant heat transfer in this region depends mainly on the particles.

Carbon was initially considered to be the most suitable seeding material. It has good absorptivity, high boiling point, and low density. Also it is available in large quantities having very small particle sizes. Recently, however, irregularities have been observed in the absorption of carbon particles in hydrogen gas during flash experiments.[3] These may arise as a result of a chemical reaction at the surface of the particles at high temperature. More information is needed to determine if carbon particles and hydrogen gas are indeed a suitable combination for gas-core, nuclear reactors. In the meantime, the use of several other materials, such as tungsten, rhenium, and tantalum, has been suggested. These materials are reported[4,5] to exhibit no significant difference in opacity at a wavelength of 0.579 micron, and all of them have a high boiling point. Also they do not react with hydrogen gas at high temperatures. However, the theoretical maximum extinction parameter for carbon at a wavelength of 0.4 micron is approximately three times that of tungsten per unit mass of powder.

Theoretical studies of radiant heat transfer to absorbing gases and aerosols have been performed by many investigators[6,7,8,9]. In general, the emitting surface and the absorbing gas were treated mathematically as

if divided into zones. For cylindrical systems, the enclosed gas was divided into right cylinders and coaxial cylindrical rings by Erkku.[7] The wall and gas were divided into zones of length equal to the diameter and called unit zones by Hoffman and Gauvin.[8] In the study of which this is a part, a complete integration was performed for cylinders from the shape of a narrow ring to that which could be considered an infinitely long conduit. Aerosol properties were also thoroughly investigated from very dilute aerosols to nearly opaque ones. These investigations sought to evaluate the radiant heat transfer from any section of the surface to any section of the aerosol, provided the surface was isothermal and the aerosol was of uniform density. Surfaces other than black were discussed.

Carbon black has been employed exclusively in recent experimental measurements. The results obtained so far have correlated well with the theoretical predictions. Tungsten powder will be used in the future to examine its absorption property and, hopefully, to obtain information on the dependence of radiant heat transfer on particle properties.

Since in an actual rocket the particles will vaporize at temperatures around or above their boiling points, it will be a problem if they disappear before the hydrogen gas becomes sufficiently absorbant. If a "window" exists in the propellant system through which the radiation may be transmitted, the container wall will be overheated. Also particles nearer the energy source may be vaporized sooner than those closer to the vessel wall. Study of the process of particle disappearance is thus needed to supply information about the "window" problem. Equipment is presently being constructed with which vaporization rate phenomenon can be observed and measured.

The objectives of this study remain mainly those of achieving a more detailed understanding of the process and mechanism of radiant heat transfer to aerosols. Experimental measurements are made to justify the various assumptions in the theoretical analysis. The results, hopefully, will be useful in reference to a number of different gaseous, nuclear, rocket concepts.

III. THEORETICAL INVESTIGATION

Theoretical studies on radiant heat transfer from a black-wall cylinder to clouds containing black particles have been reported previously.[10,11] For convenience, various view factors are introduced here for black-wall systems as well as for non-black-wall systems. The term gray body as used in this report refers to surfaces that emit and reflect diffusely.

A. Statement of the Problem

The general treatment of radiant heat transfer from a wall to a gas containing particles involves separately the energies absorbed by the carrier gas and by the suspended particles. The combination of these two factors is termed here the radiant heat transfer to the aerosol. Therefore, the absorption coefficient, k, represents the total absorption coefficient of the aerosol. In the case of an absorbing gas free of particles, k is the absorption coefficient of the absorbing gas alone. In the case of a non-absorbing gas containing absorbing particles, k is the absorption coefficient of the particles. The view factor F is defined as the fraction of energy emitted from a black surface directly incident on the receiving surface. For aerosols, the view factor F represents the fraction of energy emitted from a black surface and received by the aerosol. For gray surfaces, f is employed as the view factor. Due to the fact that infinite reflections occur in a gray-surface system, f is always larger than F for systems of the same geometry. It must be noted here that the view factors represent only the fraction of the emitted energy incident on a surface or absorbed by the aerosol. They are dimensionless and do not show by any means the magnitude of the actual heat transfer rates. The primary concern of this project is a cylindrical geometry.

B. View Factors for Black Body Systems

In general, the radiant transfer of heat from an isothermal black surface, A_w, to an aerosol near by or flowing over the surface can be expressed as

$$q_{w \to a} = A_w F_{wa} \sigma T_w^4 \tag{1}$$

where the subscript w denotes the wall surface and a the aerosol.

If the absorption coefficient of the aerosol, k, is assumed constant, the view factor from wall to the aerosol, F_{wa}, can be written for a cylindrical system as

$$F_{wa} = \frac{1}{\pi A_w} \int_{A_a} \int_{A_w} \frac{e^{-kS} \cos \beta_w \cos \beta_a}{S^2} \, dA_w \, dA_a \tag{2}$$

where S is the distance between an emitting surface element and a receiving differential volume of aerosol. β_w and β_a are the angles between the direction of the radiation and the normal direction to the surfaces of the wall and the aerosol, respectively. The quantities of equation 2 can be expressed by the coordinates shown in Figure 1 as:

$$\cos \beta_a \, dA_a = k \, dV_a = kr \, dr \, dx_a \, d\theta \tag{3}$$

$$dA_w = R \, d\Psi \, dx_w \tag{4}$$

$$\cos \beta_w = \frac{R - r \cos \Psi}{[(x_w - x_a)^2 + R^2 + r^2 - 2Rr \cos \Psi]^{1/2}} \tag{5}$$

and

$$S = [(x_w - x_a)^2 + R^2 + r^2 - 2Rr \cos \Psi]^{1/2} \tag{6}$$

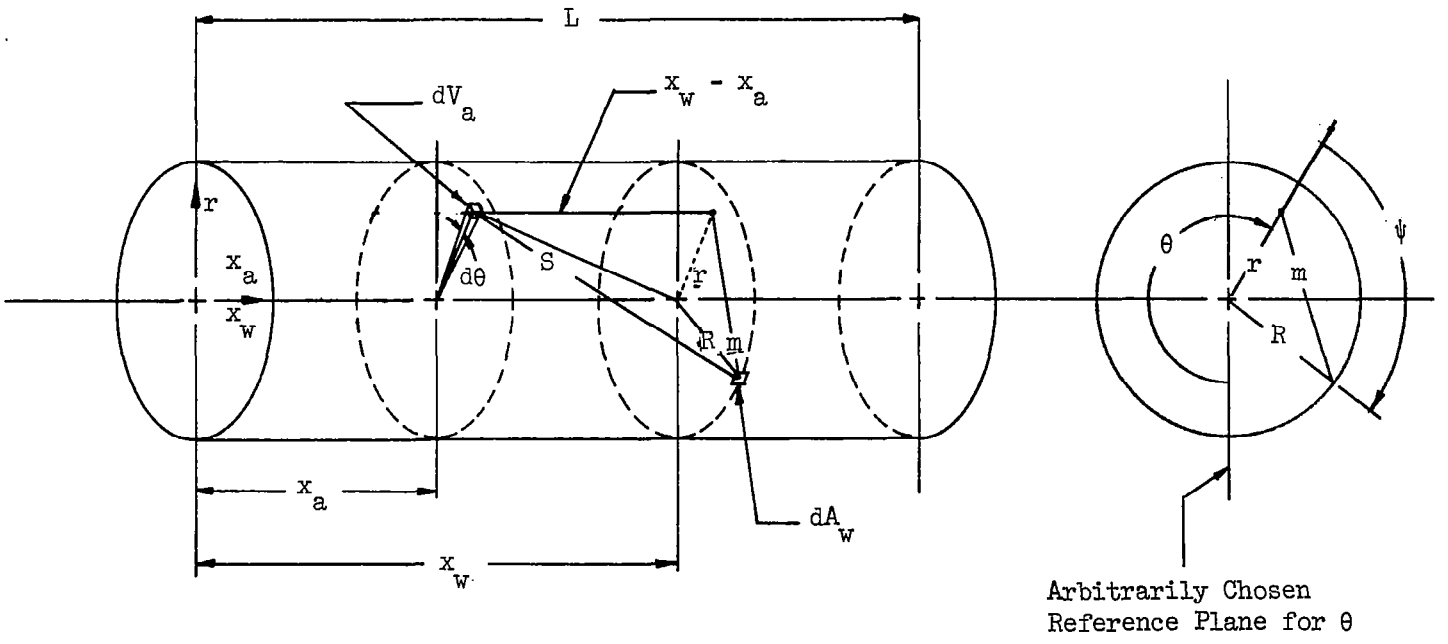

Figure 1. Definition of Geometric Variables for the Wall-to-Aerosol View Factor Formulations.

Thus equation 2 becomes

$$F_{wa} = \frac{k}{2\pi^2 L_w} \int_0^{2\pi}\int_0^{R}\int_0^{2\pi}\int_0^{L_a}\int_0^{L_w} \frac{r(R - r\cos\Psi)}{[(x_w - x_a)^2 + R^2 + r^2 - 2Rr\cos\Psi]^{3/2}}$$

$$\cdot\exp\left\{-k[(x_w - x_a)^2 + R^2 + r^2 - 2Rr\cos\Psi]^{1/2}\right\} dx_w\, dx_a\, d\Psi\, dr\, d\theta \quad (7)$$

If the absorbing aerosol is completely within the cylinder, then $L_a = L_w = L$. Thus equation 7 becomes

$$F_{wa} = \frac{k}{\pi L} \int_0^{R}\int_0^{2\pi}\int_0^{L}\int_0^{L} \frac{r(R - r\cos\Psi)}{[(x_w - x_a)^2 + R^2 + r^2 - 2Rr\cos\Psi]^{3/2}}$$

$$\cdot\exp\left\{-k[(x_w - x_a)^2 + R^2 + r^2 - 2Rr\cos\Psi]^{1/2}\right\} dx_w\, dx_a\, d\Psi\, dr \quad (8)$$

where L and R are the length and radius of the cylindrical system, respectively.

The integrations against x_w and x_a were performed analytically by means of a series expansion of the exponential term. The subsequent integrations for Ψ and r were performed numerically by use of closed-form, Newton-Cotes, quadrature formulae. The results for aerosols of various absorption parameters, kR, are presented in Figure 2 as a function of the length-to-radius ratio, L/R. The radiant heat transfer rate can be easily evaluated by inserting the value read from the figure into equation 1.

C. View Factors for Gray Body Systems

Classical radiant heat transfer problems assume black-body behavior. In general, systems existing in practice are very seldom black. Analysis of a non-black-body system is very complex, but an approximate result can be obtained

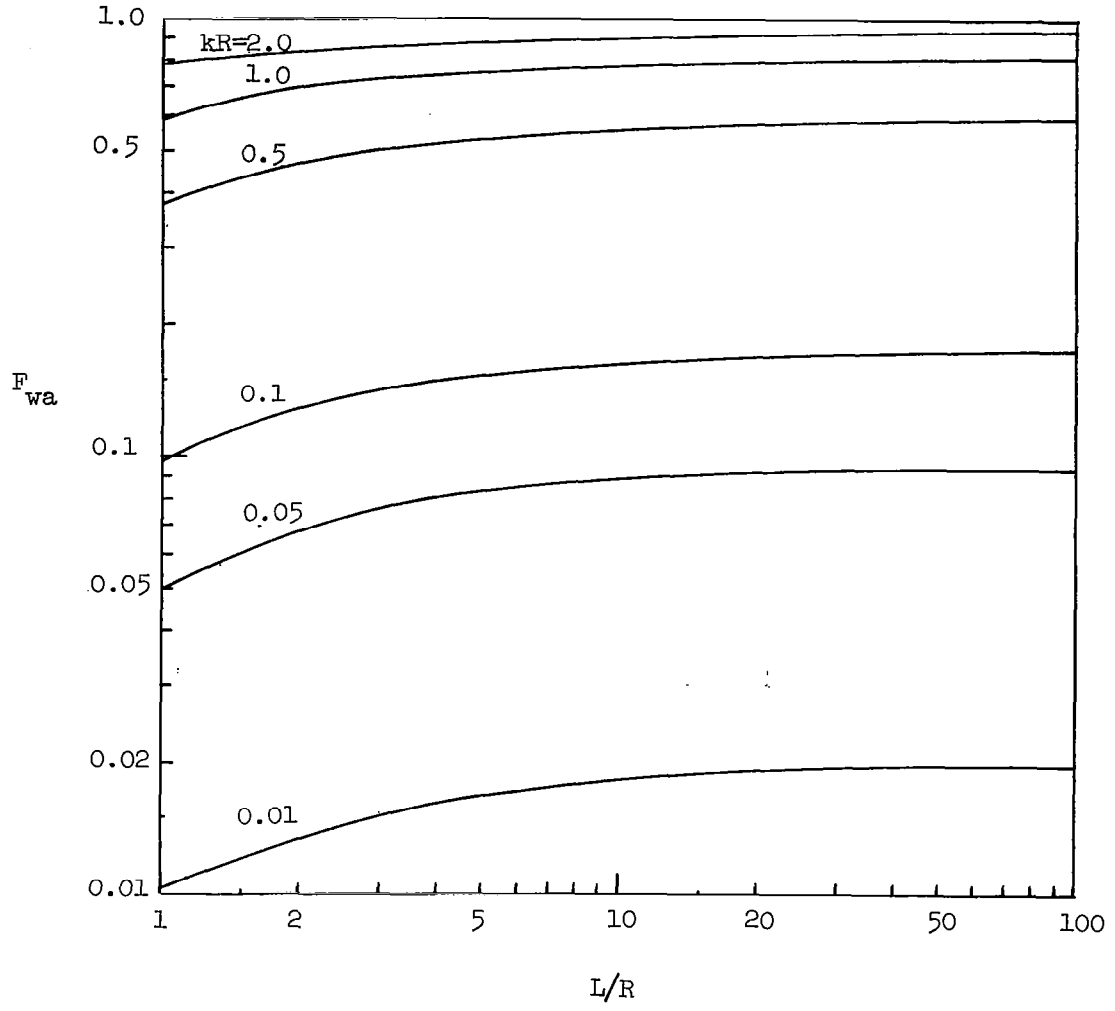

Figure 2. Wall-to-Aerosol View Factors for Black-Wall Cylinders Containing Aerosols Having Various Absorption Coefficients.

relatively easily provided assumptions are made. If a system can be assumed to have surfaces that are perfectly diffuse emitters and reflectors, the analysis can be much simplified. A surface usually can be assumed to be diffuse if it is relatively rough compared to the wavelength of the incident radiation. This means that all surfaces will behave more diffusely when the incident radiation comes from a higher temperature source with the same emitting property.

In a black-surface, cylindrical system, that portion of the radiation passing through the aerosol and reaching the wall of the cylinder is absorbed completely by the wall. But in a gray-wall system, the portion reaching the wall is partially absorbed and partially reflected. The reflected energy is available for further absorption by the aerosol. This infinitely continuing process adds to the absorption as more reflection occurs. If f_{wa} is assumed to be the view factor for the gray-surface system which includes the initial view factor and the view factors of the continuing process of reflection, then the radiant heat transfer from the wall to the aerosol can be expressed as

$$q_{w \to a} = A_w \, f_{wa} \, \epsilon \, \sigma \, T_w^4 \tag{9}$$

where ϵ is the total emissivity of the wall surface. The view factor f_{wa} can be expressed by an infinite series as

$$f_{wa} = F_{1a} + \rho \, F_{1w} \, F_{2a} + \rho^2 \, F_{1w} \, F_{2w} \, F_{3a}$$

$$+ \rho^3 \, F_{1w} \, F_{2w} \, F_{3w} \, F_{4a} + \cdots\cdots \tag{10}$$

where ρ is the reflectivity of the wall surface. The view factors, F_{1a}, F_{2a}, F_{3a}, . . . represent, respectively, the fractions of the radiant energy leaving the wall that are intercepted by the aerosol in the first pass, second pass, third pass, etc. The view factors F_{1w}, F_{2w}, F_{3w}, . . . represent the fraction of radiant energy leaving the wall that pass through the aerosol and are incident again on the wall during the first pass, second pass, third pass, etc.

A gray surface is assumed to be a perfectly diffuse emitter and reflector. Thus it may be assumed that

$$F_{1a} = F_{2a} = F_{3a} = ... = F_{wa} \tag{11}$$

and

$$F_{1w} = F_{2w} = F_{3w} = ... = F_{ww} \tag{12}$$

Equation 10 now can be reduced to

$$f_{wa} = F_{wa} [1 + \rho F_{ww} + \rho^2 F_{ww}^2 + ...] \tag{13}$$

The value of ρF_{ww} is always less than unity. Thus the expression for f_{wa} can be further simplified to

$$f_{wa} = \frac{F_{wa}}{1 - \rho F_{ww}} \tag{14}$$

Substituting f_{wa} into equation 9 gives

$$q_{w \to a} = A_w \left(\frac{\epsilon F_{wa}}{1 - \rho F_{ww}} \right) \sigma T_w^4 \tag{15}$$

The values of F_{wa} are shown in Figure 2 for various systems. To evaluate F_{ww}, the following expression

$$F_{w1w2} = \frac{1}{\pi A_w} \int_{A_{w2}} \int_{A_{w1}} \left(e^{-kS}\right) \left(\frac{\cos \beta_{w1} \cos \beta_{w2}}{S^2}\right) dA_{w1}\, dA_{w2} \tag{16}$$

may be employed, where the quantities in terms of the coordinates are:

$$dA_{w1} = R\, d\theta\, dx_{w1} \tag{17}$$

$$dA_{w2} = R\, d\Psi\, dx_{w2} \tag{18}$$

$$S = [(x_{w1} - x_{w2})^2 + 2R^2 - 2R^2 \cos \Psi]^{1/2} \tag{19}$$

and

$$\cos \beta_{w1} = \cos \beta_{w2} = \frac{R(1 - \cos \Psi)}{[(x_{w1} - x_{w2})^2 + 2R^2 - 2R^2 \cos \Psi]^{1/2}} \tag{20}$$

Since the emitter and the receiver are the same cylinder, $L_{w1} = L_{w2} = L$. Equation 16 thus becomes

$$F_{ww} = \frac{R^3}{2\pi^2 L} \int_0^{2\pi} \int_0^{2\pi} \int_0^{L} \int_0^{L} \frac{(1 - \cos \Psi)^2}{[(x_{w1} - x_{w2})^2 + 2R^2 - 2R^2 \cos \Psi]^2}$$

$$\cdot \exp \left\{-k[(x_{w1} - x_{w2})^2 + 2R^2 - 2R^2 \cos \Psi]^{1/2}\right\} dx_{w1}\, dx_{w2}\, d\Psi\, d\theta \tag{21}$$

or

$$F_{ww} = \frac{R^3}{\pi L} \int_0^{2\pi} \int_0^L \int_0^L \frac{(1 - \cos \Psi)^2}{[(x_{w1} - x_{w2})^2 + 2R^2 - 2R^2 \cos \Psi]^2}$$

$$\cdot \exp \left\{-k[(x_{w1} - x_{w2})^2 + 2R^2 - 2R^2 \cos \Psi]^{1/2}\right\} dx_{w1}\, dx_{w2}\, d\Psi \qquad (22)$$

The value of F_{ww} can be obtained similarly as stated for F_{wa} except one less integral term is involved than for F_{wa} because of the constant radius R. Hoffman and Gauvin[8] obtained solutions for cylinders of length equal to one, two, and three times that of the diameter. Their results are modified and are presented in Figure 3 with interpolation and extrapolation added.

The view factors calculated by equation 14 are nearly exact for relatively dense aerosols. For systems of dilute aerosols, very small errors are to be expected for short (length less than radius) or long (length greater than five times radius) cylinders. This results from the nearly uniform irradiation within short cylinders and the negligible end effects for long cylinders. For intermediate cylinders, the center portion receives more radiant energy per unit area than each of the end portions. For example, the center portion of a cylinder having a length equal to three times the radius receives about three per cent more of the emitted radiant energy than each of the end portions receives if the absorption parameter, kR, is assumed to be 0.1. An error analysis with consideration of this uneven irradiation for a surface of reflectivity of 0.5 was performed, and the final result showed no significant difference from that obtained by equation 14 in which the assumption of uniform irradiation was made. Apparently, the increase in absorption due to uneven irradiation is very small.

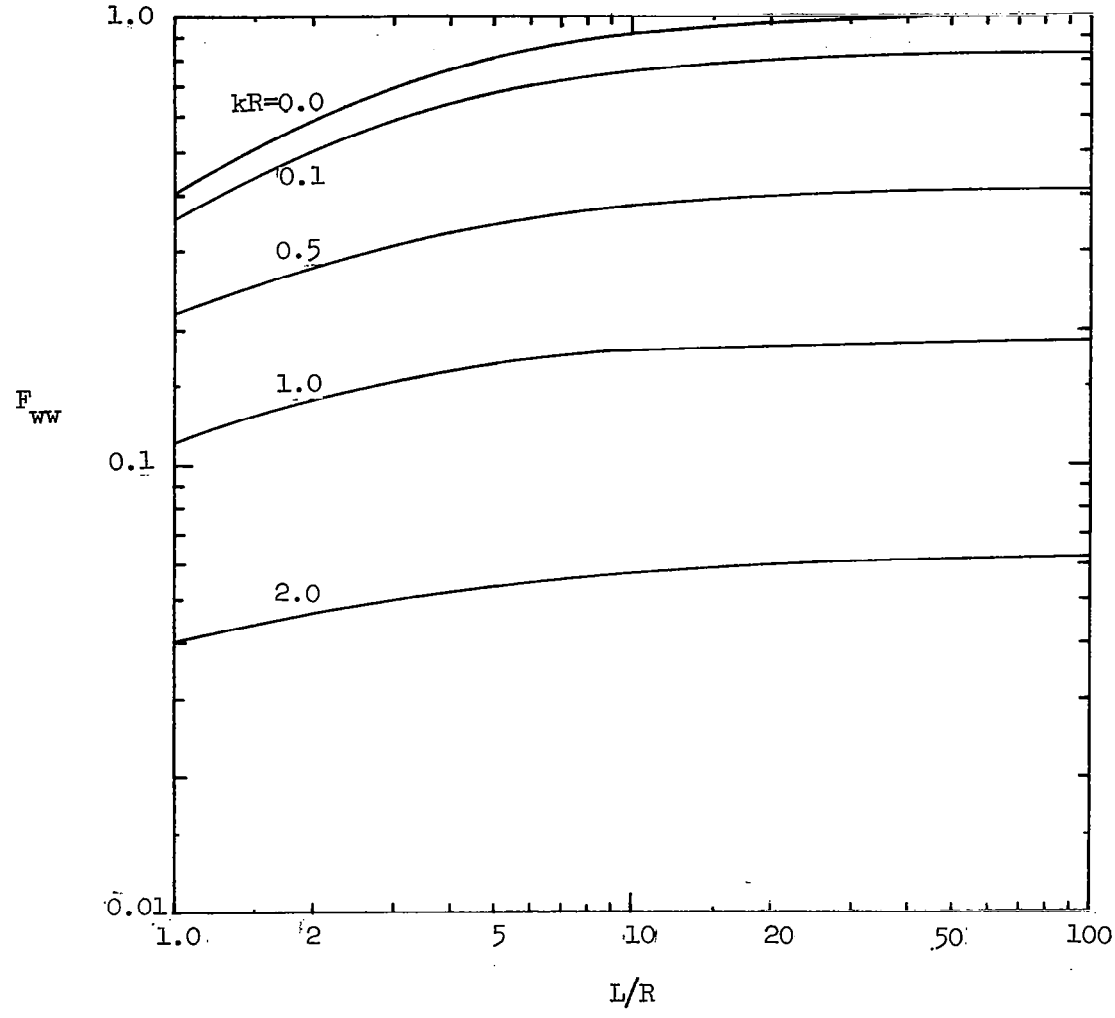

Figure 3. Wall-to-Wall View Factors for Black-Wall Cylinders Containing Aerosols Having Various Absorption Coefficients.

D. View Factors for Specular-Reflection Systems

Specular reflection refers to the process in which the angle of reflection equals the angle of incidence but with reduced intensity. Many smooth metal surfaces reflect specularly. Whether or not a surface is optically smooth depends on the wavelengths of the incident radiation. Some surfaces that appear rough to the eye may be considered smooth for long wavelength radiation. So the justification of specular reflection depends on the wavelength of the incident radiation and the relative roughness of the receiving surface. It has been stated[12,13] that a surface may be nearly a diffuse emitter even if it is a specular reflector. Here, it has been assumed that the surfaces of the cylinders are perfectly diffuse emitters and specular reflectors.

The view factors for a specular-reflection system are very difficult to evaluate analytically. The situation is unlike a diffuse-reflection surface for which the view factors of each reflection pass can be assumed to be as given by equations 10 and 14. For a cylinder of infinite length, however, the solution will be the same as for a diffuse-reflection surface. It can be shown by an analysis using an arbitrarily chosen beam of initial intensity i_o that the total absorption by the aerosol for this beam is expressed by

$$q_{i_o} = i_o(1 - e^{-kS}) + \rho\, i_o e^{-kS}(1 - e^{-kS}) + \rho^2\, i_o e^{-2kS}(1 - e^{-kS}) + \ldots.$$

$$= i_o(1 - e^{-kS})(1 + \rho e^{-kS} + \rho^2 e^{-2kS} + \ldots.)$$

$$= i_o\left(\frac{1 - e^{-kS}}{1 - \rho e^{-kS}}\right) \qquad (23)$$

where S is the distance that the arbitrarily chosen beam travels through the aerosol until it reaches the wall.

If a mean beam length, $\overline{S}$, is employed, then an overall radiant heat transfer equation may be written

$$q_{w \to a} = A_w \, \epsilon \, \sigma \, T_w^4 \left(\frac{1 - e^{-k\overline{S}}}{1 - \rho e^{-k\overline{S}}} \right) \tag{24}$$

where the view factor f'_{wa} for a specular-reflection system can be expressed by

$$f'_{wa} = \frac{1 - e^{-k\overline{S}}}{1 - \rho e^{-k\overline{S}}} \tag{25}$$

Actually, this expression is the same as equation 14 because

$$F_{wa} = 1 - e^{-k\overline{S}} \tag{26}$$

and

$$F_{ww} = e^{-k\overline{S}} \tag{27}$$

so that

$$f'_{wa} = f_{wa} = \frac{F_{wa}}{1 - \rho \, F_{ww}} \tag{28}$$

Usually, cylinders with lengths greater than ten times their radius can be safely considered as infinitely long cylinders with even dilute aerosols in them. For a cylinder having a length equal to its diameter (as was the furnace used in this study) the maximum error will be about five per cent for the

experiment with an aerosol having kR = 0.1 if the surface of the furnace is indeed a perfect specular reflector with a reflectivity of 0.5. In some practical high temperature systems, the surfaces can either be assumed to be diffuse or to behave in a manner between specular reflection and diffuse reflection. Equation 28 is believed to be a good compromise for most systems of smooth metal surfaces and fairly concentrated aerosols.

E. View Factors Among Zones

If a cylinder with a black wall is arbitrarily divided into two zones, say A and B, the view factors for each of the zones to the aerosol in its zone can be obtained from Figure 2. The view factor from the wall of zone A, w_A, to the aerosol in zone B, a_B, can be evaluated by the following equation:

$$F_{w_A \to a_B} = \frac{k}{\pi L_A} \int_0^R \int_0^{2\pi} \int_0^{L_A} \int_{L_A}^{(L_A+L_B)} \frac{r(R - r\cos\Psi)}{[(x_B - x_A)^2 + R^2 + r^2 - 2Rr\cos\Psi]^{3/2}}$$

$$\cdot \exp\left\{-k[(x_B - x_A)^2 + R^2 + r^2 - 2Rr\cos\Psi]^{1/2}\right\} dx_B\, dx_A\, d\Psi\, dr \qquad (29)$$

where L_A and L_B are the lengths of zones A and B, respectively. Both of the coordinate variables x_A and x_B are along the axis of the cylinder as shown in Figure 4.

Similarly, the view factor from the wall of zone B, w_B, to the aerosol in zone A, a_A, can be expressed by

$$F_{w_B \to a_A} = \frac{k}{\pi L_B} \int_0^R \int_0^{2\pi} \int_{L_A}^{(L_A+L_B)} \int_0^{L_A} \frac{r(R - r\cos\Psi)}{[(x_B - x_A)^2 + R^2 + r^2 - 2Rr\cos\psi]^{3/2}}$$

$$\cdot \exp\left\{-k[(x_B - x_A)^2 + R^2 + r^2 - 2Rr\cos\Psi]^{1/2}\right\} dx_A\, dx_B\, d\Psi\, dr \qquad (30)$$

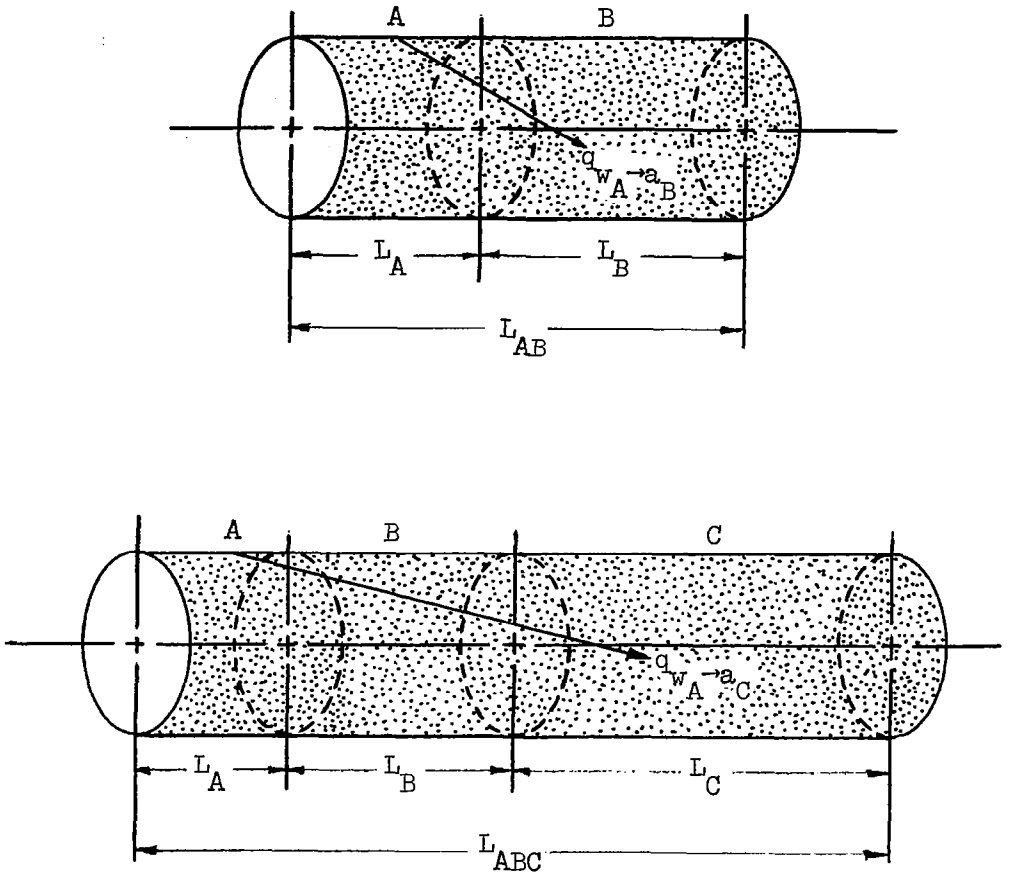

Figure 4. Radiant Heat Transfer Between Zones.
Top: Adjacent Zones Bottom: Separated Zones

If two zones are separated by a third zone, a similar equation but one with some modification is needed. In Figure 4, for example, zones A and C are separated by zone B. The view factors from the wall of zone A to the aerosol in zone C and from the wall of zone C to the aerosol in zone A can be expressed by

$$F_{w_A \to a_C} = \frac{k}{\pi L_A} \int_0^R \int_0^{2\pi} \int_0^{L_A} \int_{(L_A+L_B)}^{(L_A+L_B+L_C)} \frac{r(R - r\cos\Psi)}{[(x_C - x_A)^2 + R^2 + r^2 - 2Rr\cos\psi]^{3/2}}$$

$$\cdot \exp\left\{-k[(x_C - x_A)^2 + R^2 + r^2 - 2Rr\cos\psi]^{1/2}\right\} dx_C\, dx_A\, d\Psi\, dr \qquad (31)$$

and

$$F_{w_C \to a_A} = \frac{k}{\pi L_C} \int_0^R \int_0^{2\pi} \int_{(L_A+L_B)}^{(L_A+L_B+L_C)} \int_0^{L_A} \frac{r(R - r\cos\Psi)}{[(x_C - x_A)^2 + R^2 + r^2 - 2Rr\cos\psi]^{3/2}}$$

$$\cdot \exp\left\{-k[(x_C - x_A)^2 + R^2 + r^2 - 2Rr\cos\psi]^{1/2}\right\} dx_A\, dx_C\, d\Psi\, dr \qquad (32)$$

respectively.

By examining equations 29 and 30, 31 and 32, the following relationships are obtained:

$$A_B F_{w_B \to a_A} = A_A F_{w_A \to a_B} \qquad (33)$$

and

$$A_C F_{w_C \to a_A} = A_A F_{w_A \to a_C} \qquad (34)$$

The lengths of zones A, B, and C vary with each system. If $L_B = \alpha_B L_A$ and $L_C = \alpha_C L_A$, it follows that $L_A+L_B = (1+\alpha_B)L_A$ and $L_A+L_B+L_C = (1+\alpha_B+\alpha_C)L_A$. Then the view factors can be evaluated for various values of L_A, α_B, and α_C. This procedure is complicated and also incomplete due to the limited values of L_A selected. A method has been developed to obtain the view factors by using a simple equation.

For two adjacent cylinders, let $L_{AB} = L_A+L_B$. Then the relationship between the view factors can be expressed as

$$(AF_{wa})_{L_{AB}} = (AF_{wa})_{L_A} + (AF_{wa})_{L_B} + A_A F_{w_A \to a_B} + A_B F_{w_B \to a_A} \tag{35}$$

From equations 33 and 35, there is obtained

$$A_A F_{w_A \to a_B} = A_B F_{w_B \to a_A} = \frac{1}{2}\left[(AF_{wa})_{L_{AB}} - (AF_{wa})_{L_A} - (AF_{wa})_{L_B}\right] \tag{36}$$

or

$$L_A F_{w_A \to a_B} = L_B F_{w_B \to a_A} = \frac{1}{2}\left[L_{AB}(F_{wa})_{L_{AB}} - L_A(F_{wa})_{L_A} - L_B(F_{wa})_{L_B}\right] \tag{37}$$

The view factors F_{wa} for various length-to-radius ratios are available in Figure 2.

If two zones of interest, such as A and C in Figure 4, are not adjacent, the relationship between the view factors can be expressed by

$$L_A F_{w_A \to a_C} = L_A F_{w_A \to a_{BC}} - L_A F_{w_A \to a_B} \tag{38}$$

where a_{BC} represents the aerosol in adjacent zones B and C and can be considered

to be a single zone of length L_{BC}. Equation 38 may be reduced to

$$F_{w_A \to a_C} = F_{w_A \to a_{BC}} - F_{w_A \to a_B} \tag{39}$$

The values of $F_{w_A \to a_{BC}}$ and $F_{w_A \to a_B}$ can be evaluated by equation 36. Similarly, there is obtained

$$F_{w_C \to a_A} = F_{w_C \to a_{AB}} - F_{w_C \to a_B} \tag{40}$$

For gray-wall systems, the view factors for gray walls are used in the above equations. The values of view factors can be obtained from

$$L_A f_{w_A \to a_B} = L_B f_{w_B \to a_A} = 1/2 \left[L_{AB}(f_{wa})_{L_{AB}} - L_A(f_{wa})_{L_A} - L_B(f_{wa})_{L_B} \right] \tag{41}$$

If equation 41 is written in energy terms, it becomes

$$q_{w_A \to a_B} = 2\pi R L_A f_{w_A \to a_B} \epsilon \sigma T_w^4 \tag{42}$$

The quantity, $q_{w_A \to a_B}$, includes the radiation emitted and reflected from the wall of section A and absorbed directly by the aerosol in section B plus that portion of absorbed energy reflected by the wall of section B but originally emitted and reflected from the wall of section A. In other words, the quantity $q_{w_A \to a_B}$ represents the additional portion of absorption due to the presence of section A.

IV. EXPERIMENTAL INVESTIGATIONS

In earlier phases of this study, a furnace of Kanthal wire (Kanthal Company, Stanford, Connecticut) was employed as the source of radiant energy. Various particle clouds were passed through a quartz conduit inside the furnace.[10,11] Measurements of heat transfer were made at a furnace temperature of 2280°F. The results agreed very well with the theoretical predictions. Total heat transfer rates only up to 8 Btu/min were recorded due to the upper temperature limit of the furnace. A new furnace was designed in order to extend the temperature range of the experiments and also to confirm the theoretical predictions at higher temperatures. At the same time, highly absorbing aerosols were generated so that the efficiency of transfer was increased from the previous high of 16 per cent to 60 per cent of the total radiant energy emitted. The highest temperature attained to date is 3850°F, but achieving higher temperatures is still a goal. A new cloud generator has been designed, and future tests will be performed at higher particle concentrations.

A. General Operation

The present heat transfer apparatus consists of the following basic sections: a high output power supply and control, a tungsten-element furnace with a cylindrical heater, an aerosol generator, a transmissivity-measurement set-up, particle-concentration sampler, thermocouples, and an optical pyrometer.

To make a test, the recorder and photometer are first turned on and allowed to achieve steady-state conditions. The powder is dried in advance of a test to eliminate moisture, for, otherwise, the feeder will not operate normally. Next the cooling nitrogen gas and water are turned on. The nitrogen gas is directed at the neck of the heating element where failure

would tend to occur otherwise. Water is used to cool the furnace jacket. A small portion of the nitrogen gas flow is used to keep aerosol out of the photometer slits. The carrier gas, also nitrogen, is then set at the desired flow rate with a rotameter. After this flow rate is established, the carrier gas stream is switched so as to bypass the rotameter to avoid its plugging with aerosol during the test. The nitrogen gas is allowed to flow for a few minutes to purge oxygen from the system. The surge tank is always sealed off so that there will be little oxygen in the system at the start.

The main power supply is turned on with a shorting bar placed between the two electrodes as insurance against an initial voltage surge that could damage the furnace heating element. Then the shorting bar is removed. The power controller supply is then activated, and the power level is brought up slowly until the desired temperature is achieved; the recorder is monitoring the temperature all the while. The temperature measurements from all thermocouples plotted on the recorder will ultimately reach a steady state. Then the particle feeder is turned on. The aerosol is introduced first into the surge tank and then fed to the furnace. The desired particle concentration is detected by the photometer and adjustments are made, if necessary. The temperature indications will then attain another steady state giving the data necessary for heat transfer calculations. The system is shut down following a procedure that is the reverse of that just outlined except that the cooling system usually is allowed to operate a few minutes longer to protect the apparatus.

The aerosol is sampled occasionally and the collection weighed to maintain a check on the feeder operation. Little or no change is ever

detected if the feeder is not disturbed or a setting changed.

A general view of the furnace and its arrangement are shown in Figure 5.

B. Power Supply and Main Control Panel

The power supply of the system can deliver a single-phase current of up to 1200 amperes at 480 volts. The input to the furnace is controlled by a saturable-core reactor, having a capacity of 125 kilowatts. Control of the reactor is achieved with a solid-state circuit that, at full power, delivers 6 amperes and 75 volts of saturating direct current. The alternating power level is monitored by a precision ac ammeter and kilowatt meter. The kilowatt meter allows the operator to set the power input precisely at the desired level. By recording the voltage and amperage levels during a test, the resistance of the furnace under the test condition can be calculated. These values serve to give a check on the furnace temperatures since an optical pyrometer was calibrated for this purpose. The power control panel and a temperature recorder are shown in Figure 6.

C. Improvements in the Furnace Assembly

The furnace assembly was described previously in some detail in the Semiannual Status Report No. 8. Several minor changes have been made since then to permit better overall data collection and to increase efficiency. The gas (or aerosol) flow has been channeled so that it travels only inside the heating element. The previous design allowed a small portion of this stream to pass through the annulus between the heating element and the shields. The new flow arrangement was accomplished by placing a flat tungsten ring across the annulus at the inlet of the furnace. A tube was also installed to blow cool nitrogen gas at the neck of the heating element to prevent burnout at that place.

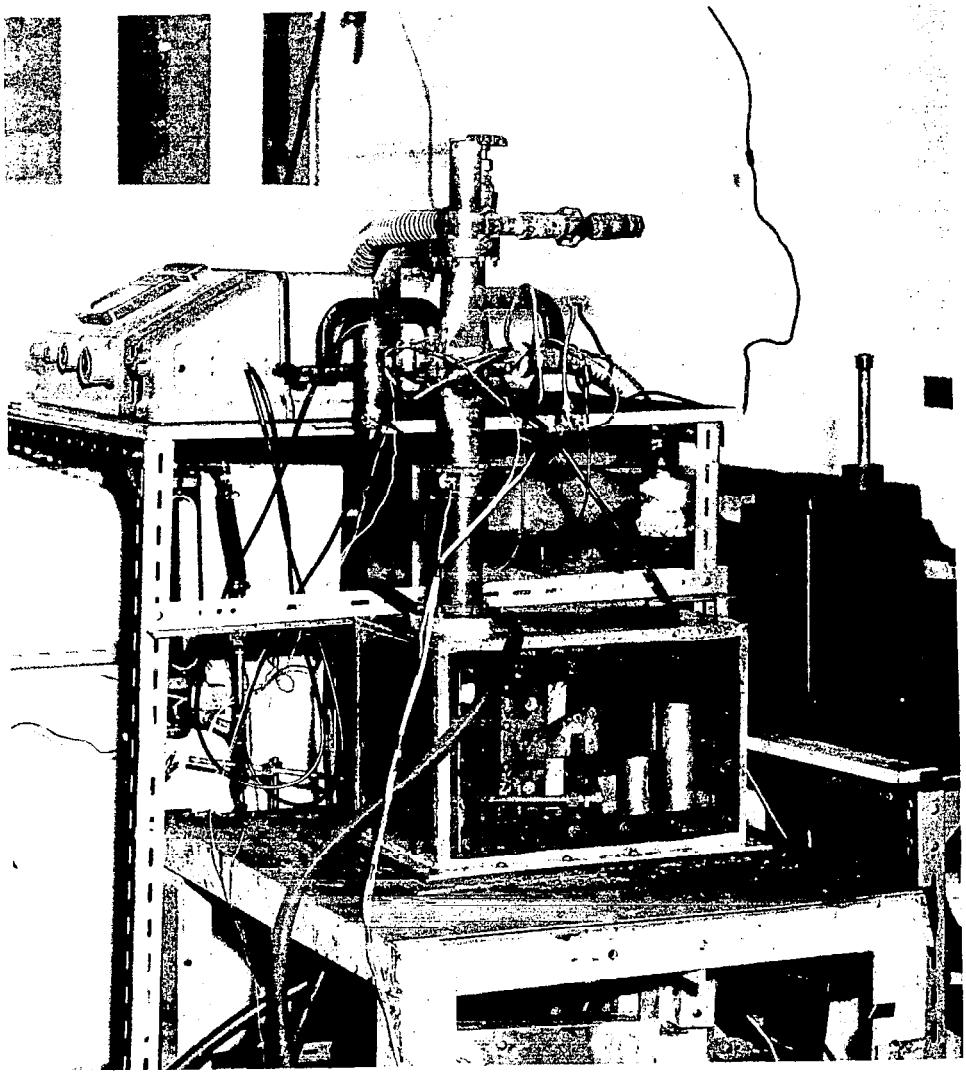

Figure 5. Photograph of the Furnace and Its Arrangement.

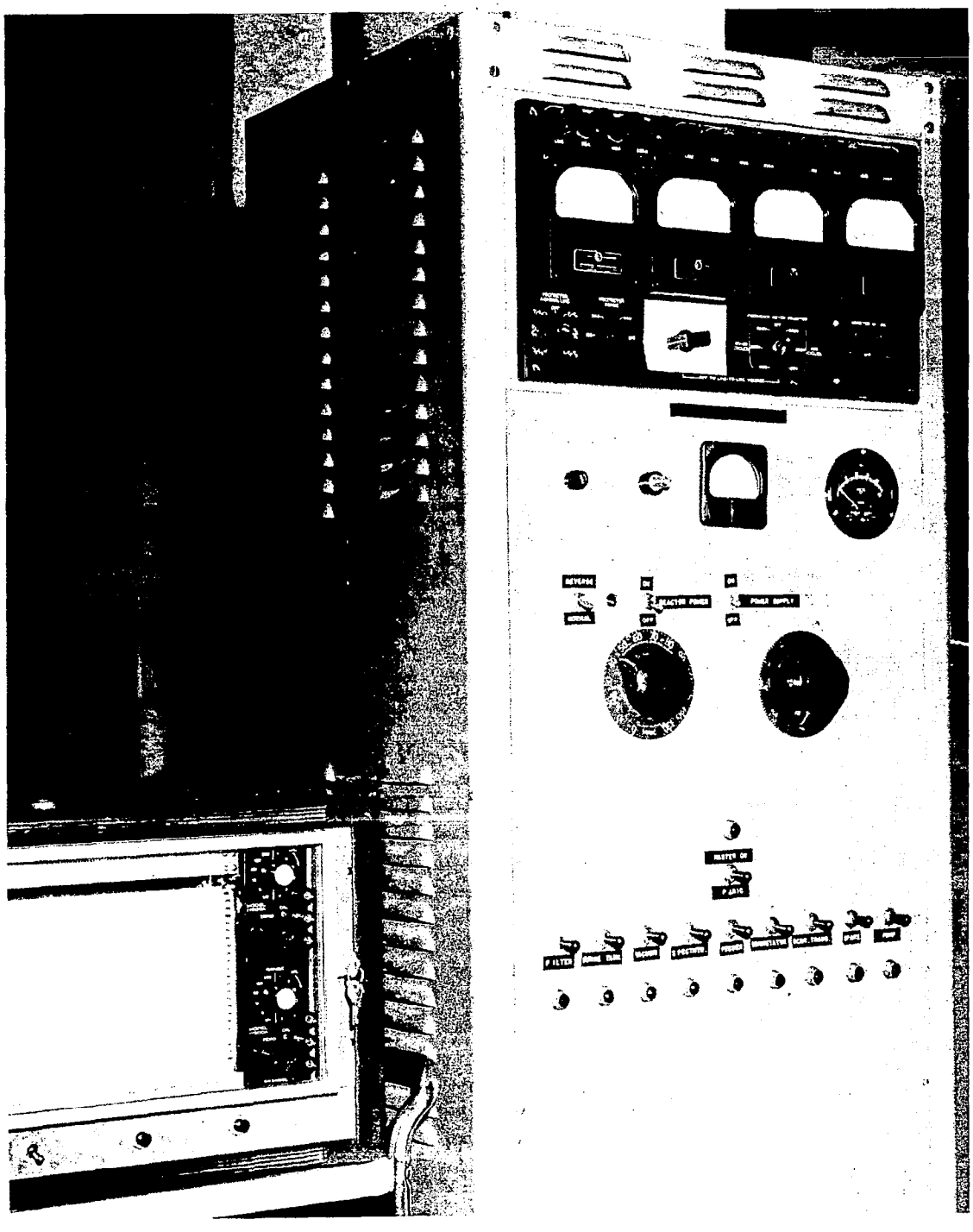

Figure 6. Photograph of the Power Control and a Temperature Recorder.

The resistance of the present heating element is much lower than before. It is so low that the reactor is overloaded when heating the furnace to temperatures above 3500°F. In an attempt to overcome this problem, a heating element was segmented in such a way that its resistance was increased nine times. The life of this heating element was short, however. It has been found that the reactor is not damaged due to overloading if the furnace is operated for a relatively short period of time. This is the procedure being employed.

D. Preparation of Particle Clouds

It is very difficult to produce a dense carbon black aerosol of uniform concentration with good dispersion. The feeder discribed in Semiannual Status Report No. 6 produced well-dispersed aerosols of limited concentration. Several unsuccessful attempts were made to fabricate improved devices before a measure of success was achieved. The most satisfactory device yet is built on the principle of an aspirator with a high velocity gas passing over a small tube and incorporating a high-speed stirring blade at the bottom of the powder chamber. A pressure equalizer and valve is included so that a slight positive pressure can be kept always in the powder chamber. By regulating the valve, the amount of powder flow can be controlled also. The output from this feeder is visually quite uniform but fluctuations can still be detected with the photometer. To overcome this the aerosols are passed through a large surge tank incorporating a fan. The aerosols emerging from this tank are very uniform.

Still another feeder is being built. Greater uniformity and increased capacity for denser aerosols is the objective. This latest design mainly

utilizes a pressurized tank and a higher speed stirrer. The capacity is expected to be increased about ten times. The particles are suspended in the container by the stirrer and then the aerosol is drawn out through a valve. Hopefully the aerosol can be used directly or diluted by addition of carrier gas. The design of the new aerosol generator is shown in Figure 7.

The most critical part of this design is the seal about the rotating shaft. Previous experience indicates, however, that the shaft can be sealed for use up to 1000 psig with no difficulty. The positions of the stirrer blades will be adjustable, and the blades will be interchangeable for adaption to various materials. The blades will be made in various shapes, some like the blades of a fan and some more like a scraper.

E. Measurements of Aerosol Properties

The aerosol properties of interest are optical density, or transmissivity, and particle load. The former is used to evaluate the absorption coefficient of the aerosol and the latter to clarify the degree of dispersion and the amount of powder required to absorb a desired amount of radiant energy.

To measure the transmissivities of the aerosols, a Beckman, Model B, spectrophotometer was used initially. It was difficult to keep the windows clean in the standard system, however. A fourteen-inch long by two-inch inside diameter circular section with a rectangular cross-section midway has been installed on the furnace outlet. The lamp and photo cell were then physically removed from the spectrophotometer and placed in specially fabricated, air-flushed housings at the ends of the extension. A thermocouple was installed near the center of light beam passage so that the aerosol temperature could be measured as it passed through the extension. This temperature will be

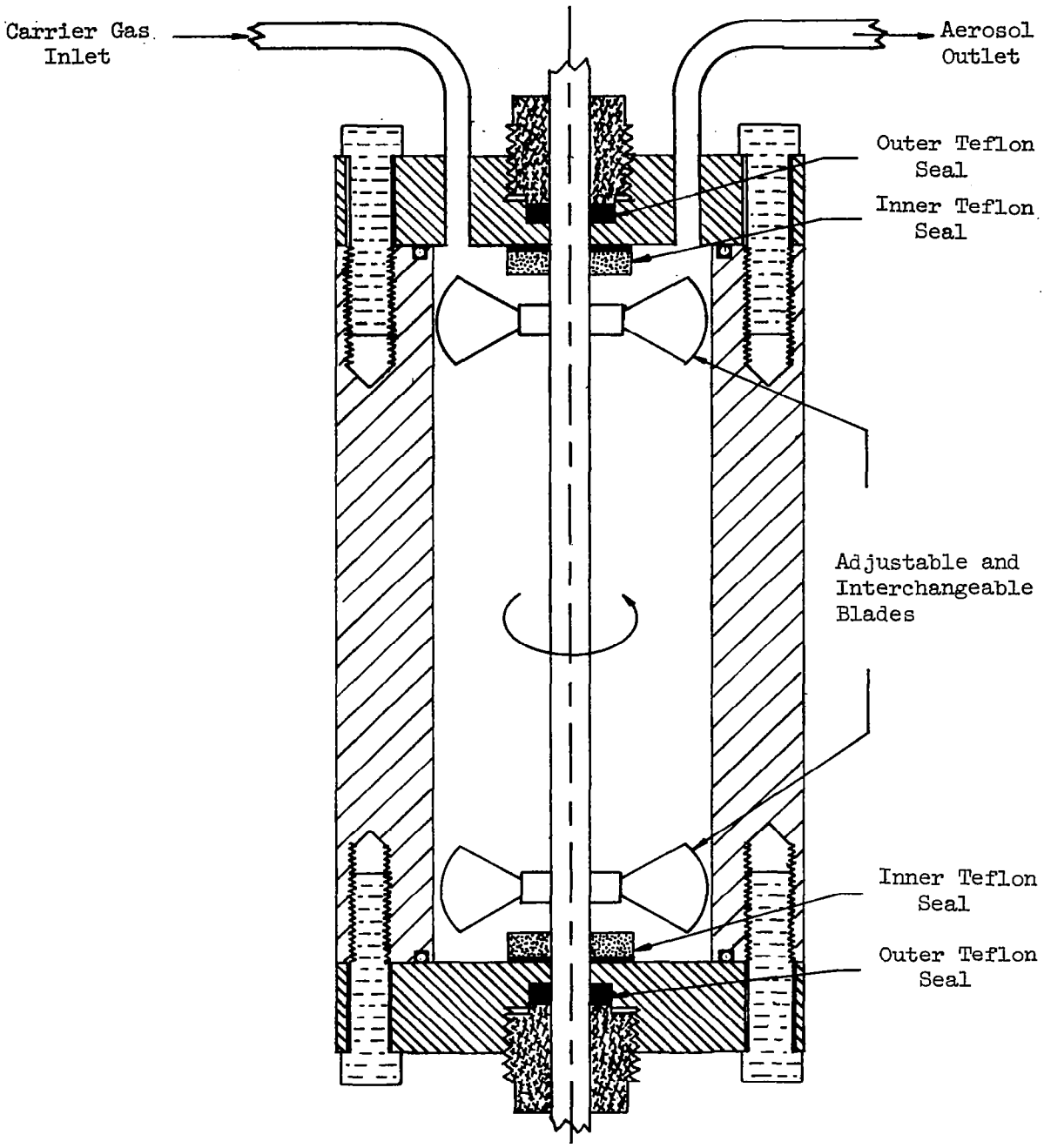

Figure 7. Aerosol Generator with Stirring Mechanism.

used to obtain the true absorption coefficient inside the furnace.

Two methods have been employed to evaluate the particle concentration of the aerosols. One utilizes Greenberg-Smith impingers as collectors and a calibrated centrifugal pump. Another employs thimble filters instead of the impingers. Samples are taken from the gas stream only when steady-state aerosol flow has been established. With the impinger method, a small amount of detergent is added to the water to aid in the wetting and collection of the particles. The collected matter is recovered by filtering the water through a millipore filter and weighing. For the thimble filter method, the moisture content of the filter itself is significant in comparison to the weight of the collected particles. The filters are dried in an oven at identical temperatures before and after the sampling to avoid errors due to a weight change of the filters themselves.

F. Temperature Measurements

The main sources of error in measuring the temperature of a gas by means of a thermocouple are (1) the exchange of radiation between the thermocouple and the surroundings, (2) the rate of heat flow along the thermocouple and the gas by convection, and (3) the rate of heat flow along the thermocouple leads by conduction. A protective shield on a thermocouple reduces the radiation exchange mainly to that between the shield and the thermocouple. The reduction differs with the geometry and radiation properties of the system and the shields. Fishenden and Saunders[14] and Bosanquet[15] discussed the wall effect in gas temperature measurements with a thermocouple. McAdams[16] also suggested a few methods of calculating the true gas temperature.

In this study, the measurements of aerosol temperature were made by

installing three sets of two thermocouples each located symmetrically about the heating element, i.e., so that both of the thermocouples of each set will receive the same amount of radiation from the heating element if the latter is heated uniformly. Thus it can be assumed that the error will be approximately identical for the thermocouples of a set. The thermocouples were installed at the locations within the furnace shown in Figure 8.

Initially, the thermocouples were all of chromel-alumel and were not shielded. Soon it was found that thermocouple No. 5 always failed when the furnace temperature was raised above 3500°F. Those thermocouples near the heating element were replaced by platinum-platinum rhodium ones and shielded by rolled platinum covers. Various shapes of shields have been tested; the latest is cone-shaped. At the small end of the cone, a round hole of about 1/8-inch diameter was made. This hole allows flow to pass the thermocouple but stops all direct radiation from the heating element.

The experimental measurements given in this report were made with thermocouples shielded so as to block more than 80 per cent of the incident radiation. The shields were made as nearly identical as they could be so that an equal temperature error could be assumed, the difference in the temperature of the aerosol entering and leaving being the major concern. As designated on Figure 8, the average value of the difference between thermocouples Nos. 1 and 4, and Nos. 2 and 5 was used as the temperature gain of the aerosol. These two values were usually very close to one another. In case thermocouple No. 5 failed or was moved to another position, the temperature difference between Nos. 1 and 4 alone could be used for the calculation. Thermocouples Nos. 3 and 6 detect the least error due to radiation, so their indications were used to estimate the absolute temperature of the aerosol in the furnace.

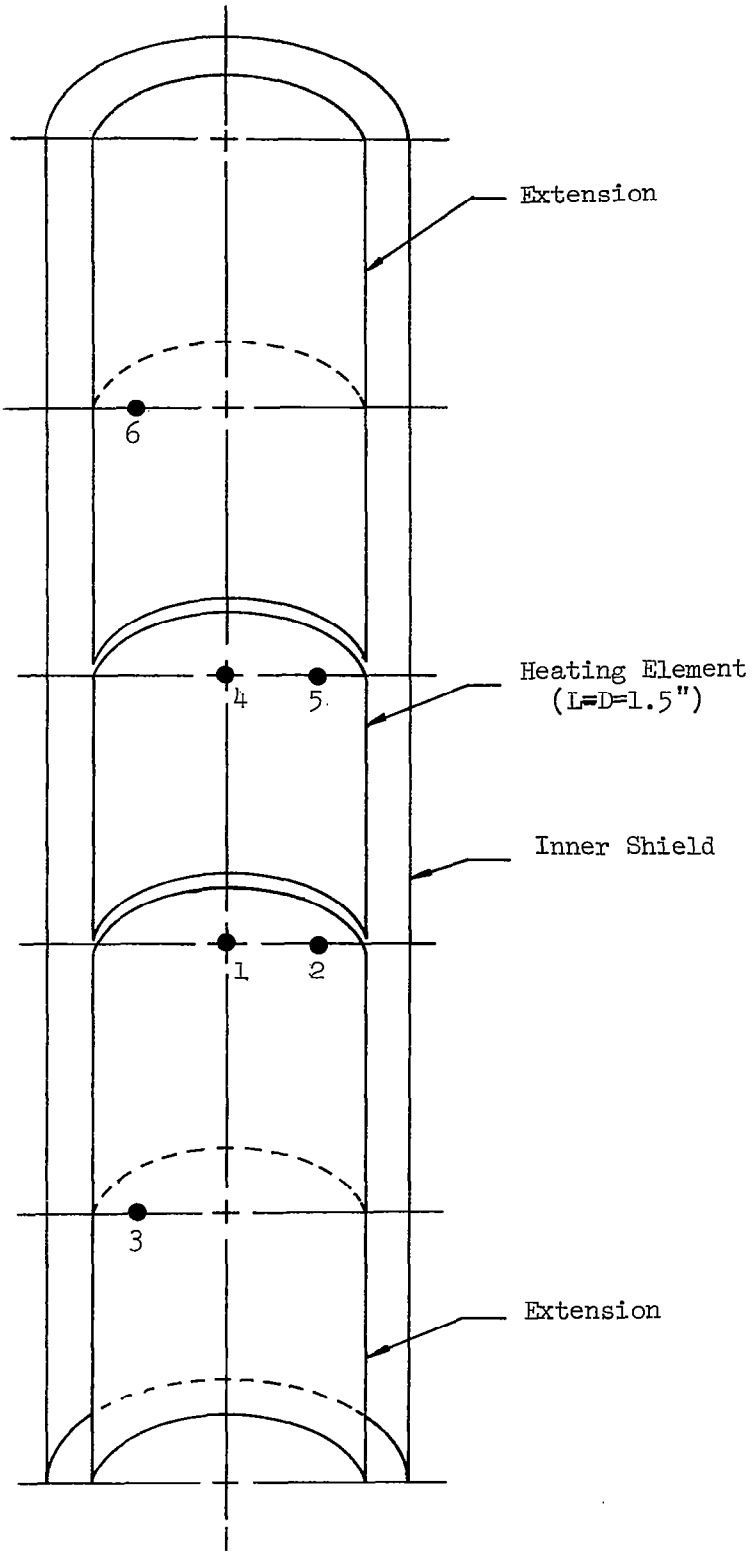

Figure 8. Positions of Thermocouples Inside the Furnace.

V. ANALYSIS OF RESULTS

A. Radiation Properties of the Heating Element

An examination on the radiant properties of tungsten was made to support the assumption of angular independence of emissivity and reflectivity. Fresnel's equations are valid for a smooth and homogeneous surface. The main factors affecting the radiant properties are the index of refraction, n, and the absorption coefficient, k. The values of n and k for tungsten are 3.47 and 3.26, respectively[13,17] for incident radiation of wavelength 0.5893 micron. The angular reflectivity, $\rho(\Phi)$, is one half the sum of the angular reflectivities on the plane of incidence and the plane normal to the plane of incidence with nitrogen gas as the medium for which the index of refraction is one. The angular reflectivities of tungsten are calculated to be as given on Figure 9 using values reported by Holl.[17] If the general Kirchhoff-law relationship applies, the angular emissivities of tungsten can be evaluated with the results being as shown by Figure 10. The values of the monochromatic emissive power of a tungsten surface and a black surface at $4300^{\circ}R$ are plotted for comparison in Figure 11. The assumption of diffuse emission for a tungsten surface is believed justified on the basis of Figures 9, 10, and 11. Whether or not a tungsten surface reflects diffusely depends also on the roughness of the surface and the property of the incident radiation. As discussed in Section III, deviation from diffuse reflection has far less influence on the results than has deviation from diffuse emission.

The values of total emissivity of tungsten were obtained from the Handbook of Chemistry and Physics. There are very little differences between these values and those reported elsewhere.[18]

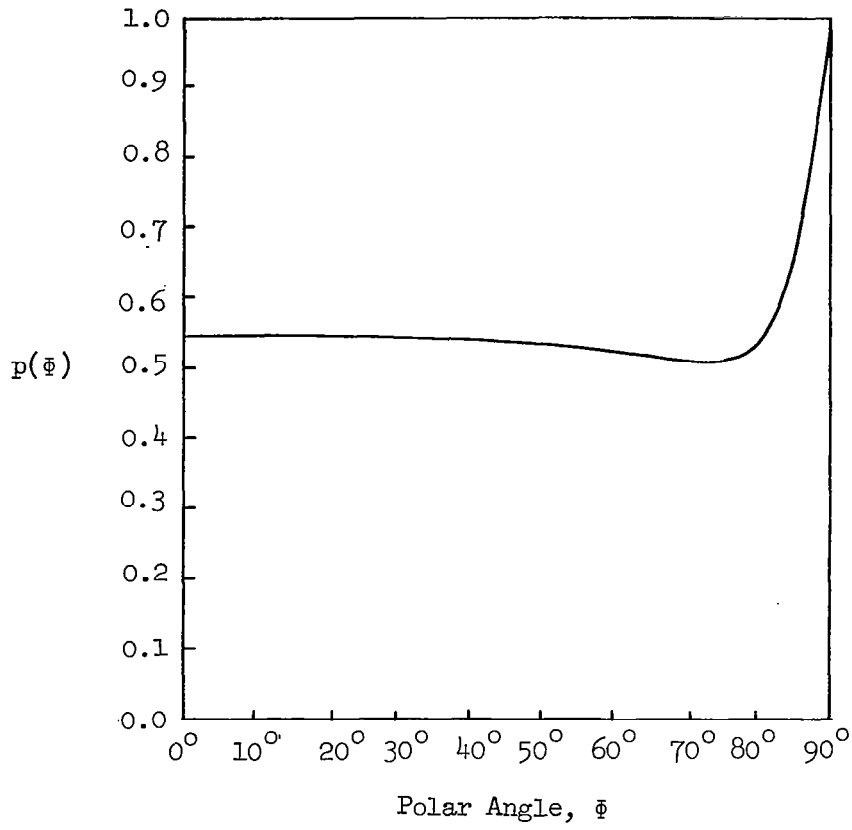

Figure 9. Angular Reflectivity of Tungsten When the Wavelength of the Incident Radiation Is 0.5893 Micron.

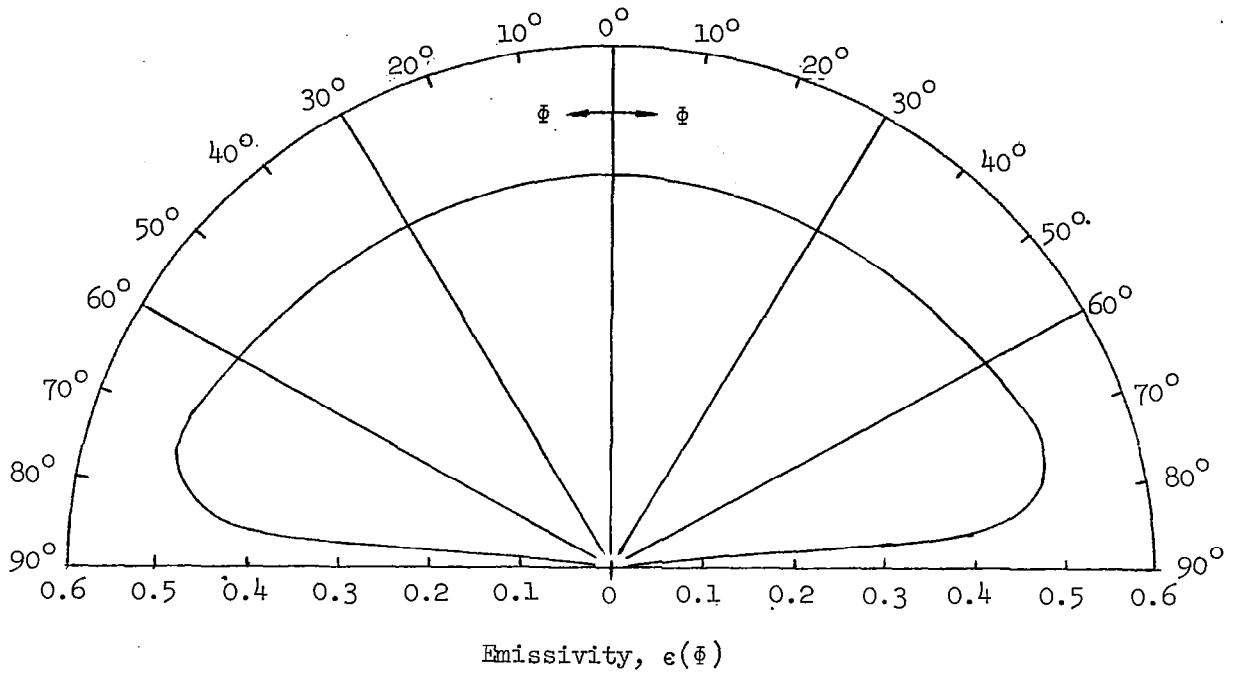

Figure 10. Angular Emissivity of Tungsten When the Wavelength of the Incident Radiation Is 0.5893 Micron.

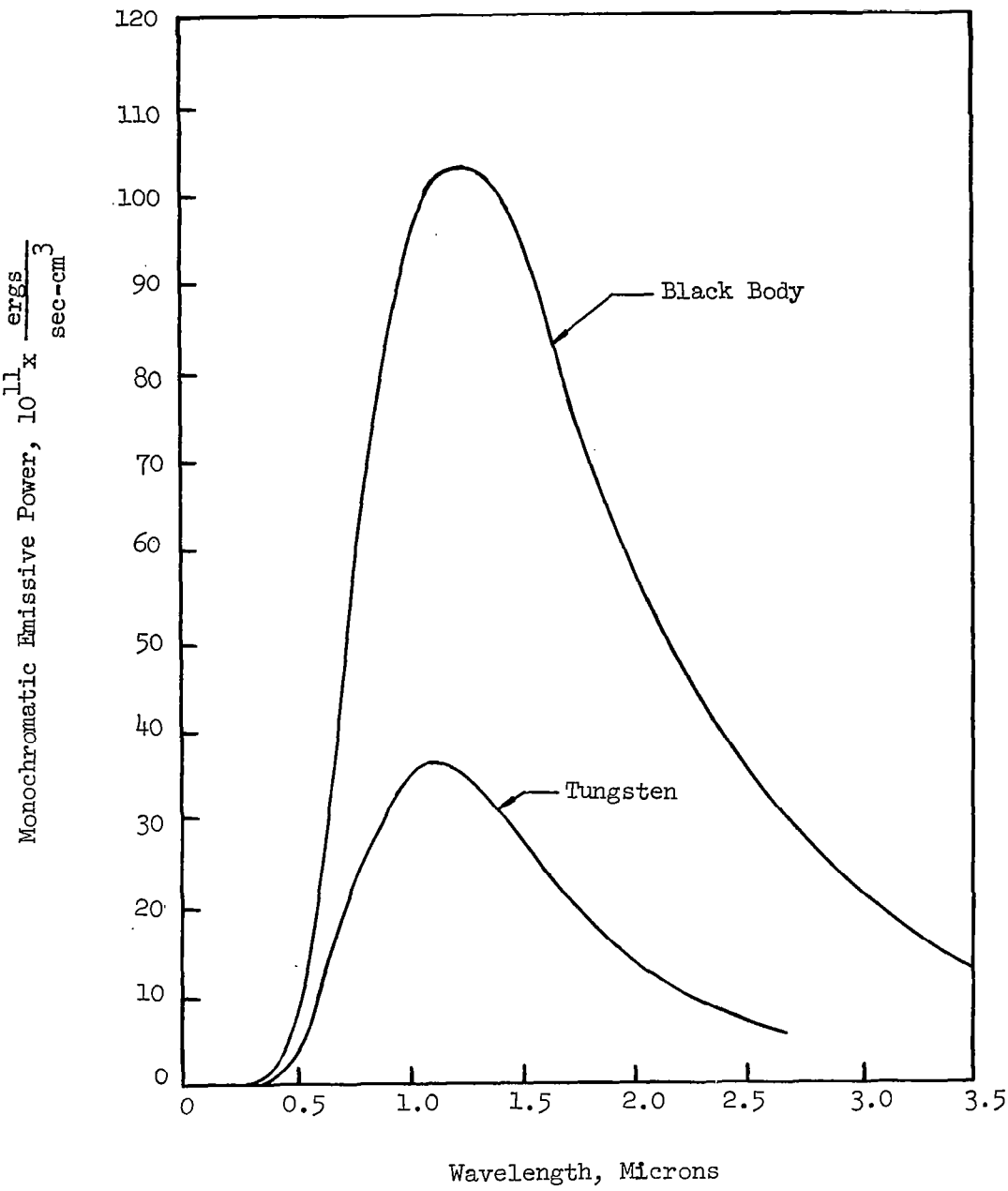

Figure 11. Monochromatic Emissive Power of a Tungsten Surface and a Black Surface at 4300°R.

B. Radiant Heat Transfer Results

The total radiant energy emitted from the inside wall of the cylindrical heating element was calculated by

$$q_e = A_w \epsilon \sigma T_w^4 \tag{41}$$

where A_w is the area of the inside surface of the cylindrical wall (= $2\pi RL$).

The value of the total energy emitted from the inside wall, q_e, is shown as a function of wall temperature T_w on Figure 12. The absorption efficiency of the aerosol, γ, is defined as the portion of emitted radiation absorbed by the aerosol. Thus the radiant heat transfer can be calculated by multiplying the emitted energy of the wall by the absorption efficiency of the aerosol.

Radiant heat-transfer rates were obtained by subtracting the heat-transfer rates by conduction and convection from the measured overall values. A blank test, or one with no particles seeded, was made prior to each test when particles were added. This approach is not quite ideal because the temperature of the gas medium is not exactly the same between unseeded and seeded gas at a given location inside the furnace. Fortunately, the temperature measurements showed that the mean temperature difference between the wall and the gas medium was nearly the same in both cases. This is to be expected because the entrance temperature of the gas is somewhat higher when unseeded than when seeded due to more radiant energy being transferred beyond the limits of the furnace. The results are presented in Figures 13 and 14. The theoretical curves are based on the assumption that a tungsten surface behaves like a gray body. The difference between the 3500°R and 4600°R

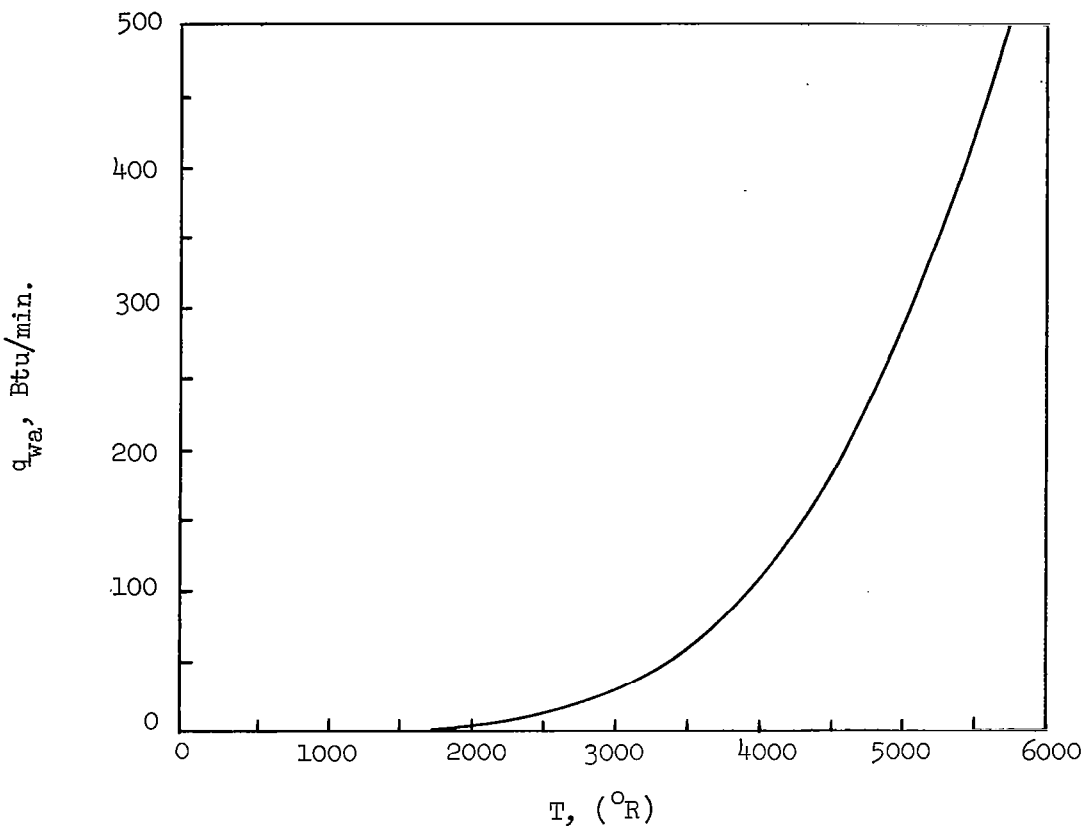

Figure 12. Total Radiant Energy Emitted from the Inside Wall of a Tungsten Cylinder with L = D = 1.5 in.

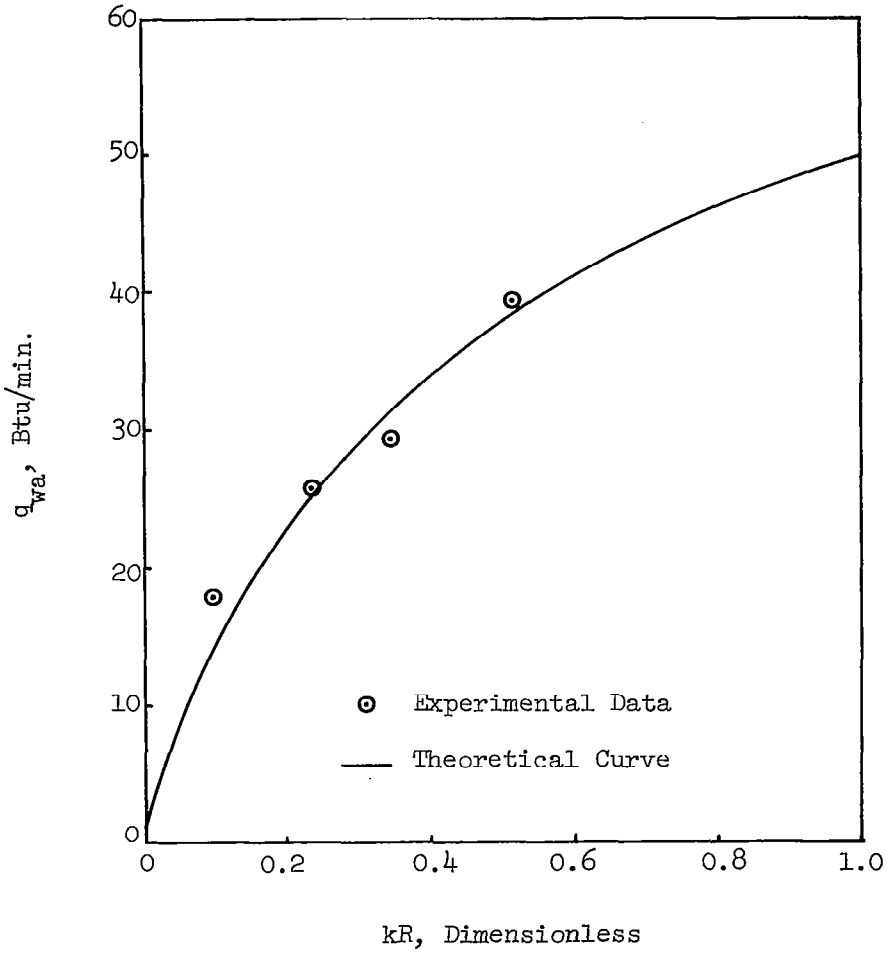

Figure 13. Rate of Radiant Energy Absorption by Carbon Black Aerosols in a Cylindrical Tungsten Furnace at 3670°R. (L = D = 1.5 in.)

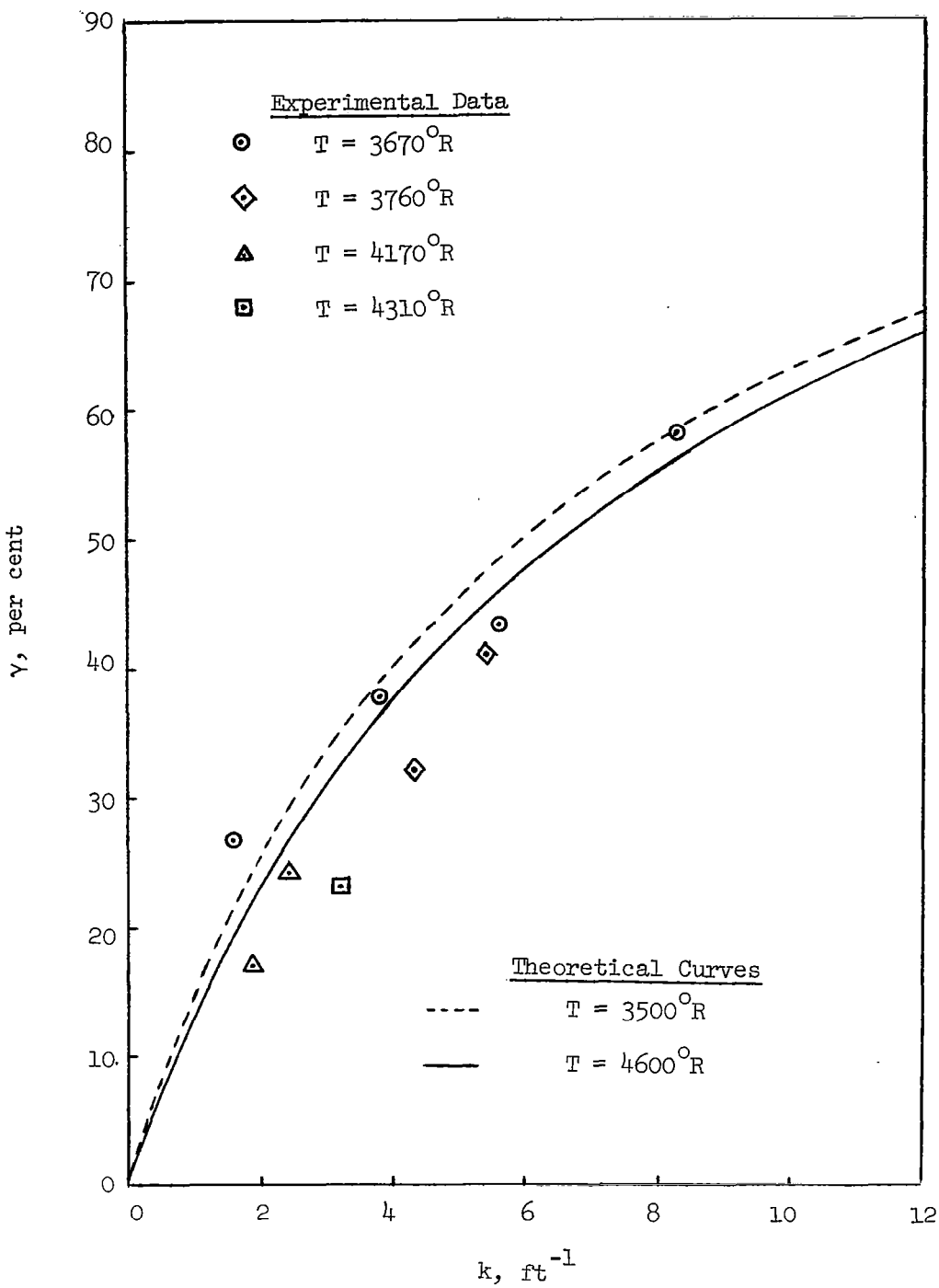

Figure 14. Absorption Efficiency of Carbon Black Aerosols in a Cylindrical Tungsten Furnace. (L = D = 1.5 in.)

curves in Figure 14 is due to the difference in emissivity and reflectivity. In general, surfaces with lesser emissivities but greater reflectivities give greater efficiencies but lesser overall radiant-heat-transfer rates. This is due to the fact that initial radiations emitted from those surfaces are less.

VI. STUDY OF PARTICLE DISAPPEARANCE IN RADIANT FIELDS

If particles are used to seed the propellant in some future gaseous-core, nuclear rocket, the lifetime and vaporization or sublimation rates of the particles must be well understood. The particles must not lose their absorption function before the propellant gas itself reaches a high temperature and becomes sufficiently absorbant. If a so-called "window" exists in the propellant system the vessel wall may be damaged. Theoretically, this rate of disappearance is a very complex problem involving simultaneously momentum, heat, and mass transfer. The heat transfer rate is the most important part and it involves conduction, convection, and radiation, the latter being of major concern. The properties of the aerosol mainly involve the concentration and size distribution of the particles; these factors will vary both radially and longitudinally in a furnace if the particles are vaporizing or sublimating. It is expected that a boundary will be formed within the aerosol on one side of which there will be no particles.

Williams[19] studied the vaporization of mist by radiation by assuming uniform radiant energy flux, steady state, and the particles to be nearly transparent spheres. This analysis gives a good starting place for this study. Other sources[9,20] utilizing much simplified conditions are available. No information concerning vaporization and sublimation occuring in a flowing aerosol has been found in the literature.

Equipment for this study that is now being assembled includes a high temperature tungsten furnace incorporating a transparent conduit of square cross-section as shown in Figure 15. Figure 16 shows a top view of the furnace. The wall of the conduit will be partially coated black so that

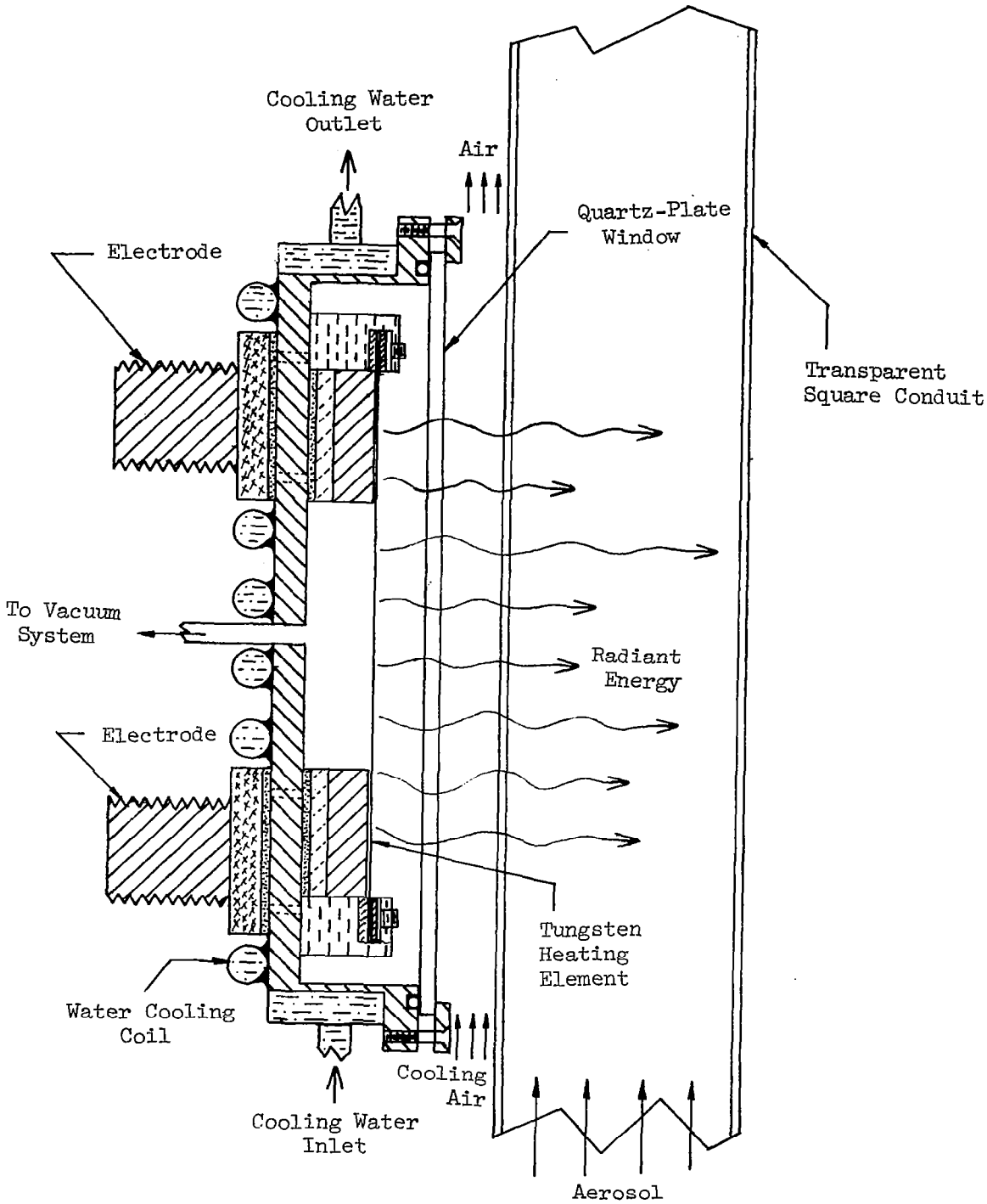

Figure 15. Experimental Apparatus for Particle Disappearance Study.

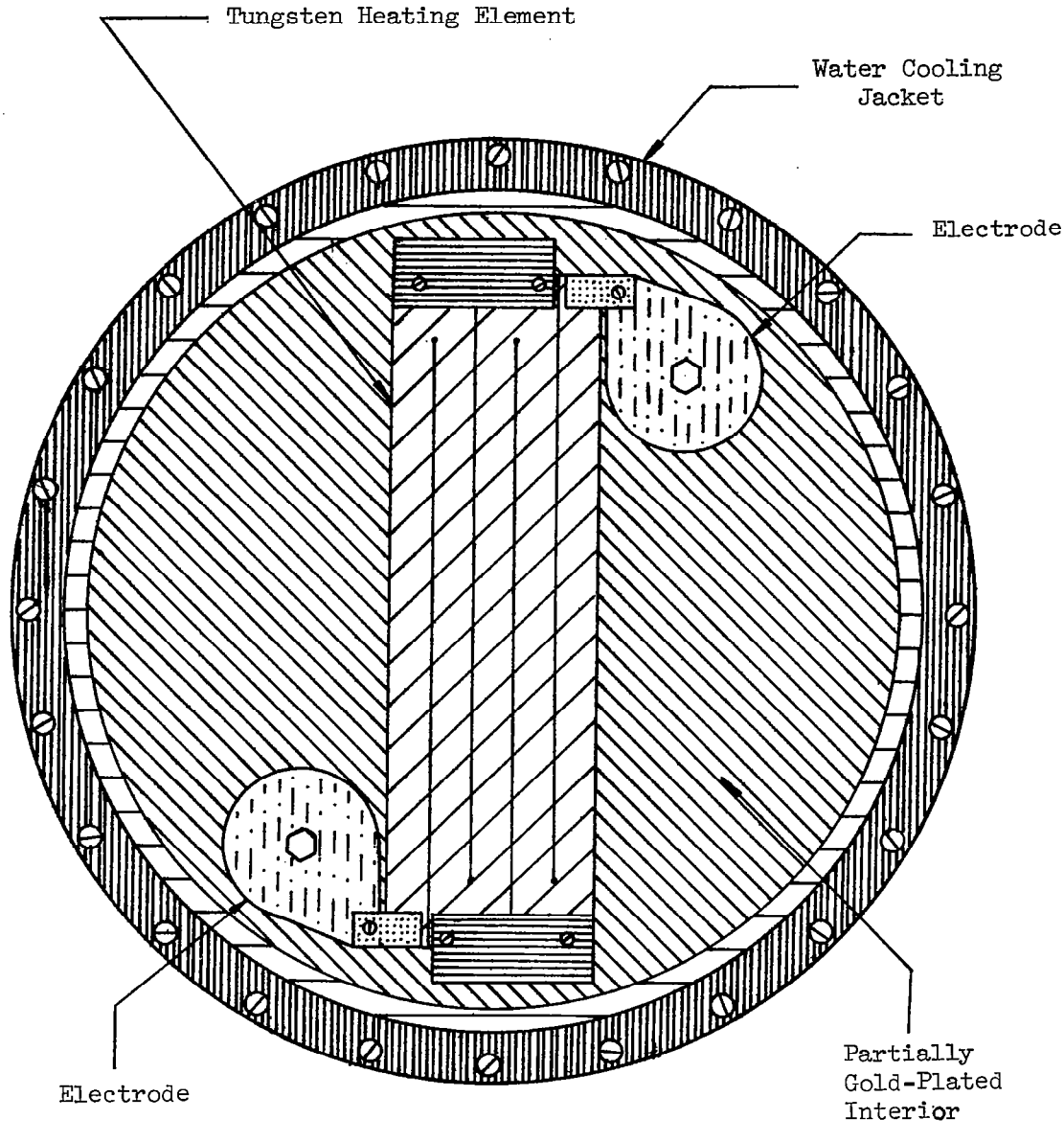

Figure 16. Top View of the Furnace for Particle Disappearance Study.

transmissivities can be measured at various locations. The transparent wall facing the furnace is air cooled to reduce the heat transfer by conduction and convection to the aerosol. A temperature distribution of the aerosol will be determined by inserting a group of thermocouples inside the conduit. Particle size distribution can be determined by isokinetic sampling of the aerosol at various locations. Droplets formed by absorbing liquids then solid particles will be tested.

VII. CONCLUDING REMARKS

1. The rate of radiant heat transfer to particle-seeded gases has been investigated theoretically for a cylindrical system. The method can be adapted to obtain solutions for annular geometries as found desirable in future nuclear rocket conceptual studies.
2. Equations are given for calculating the rate of radiant heat transfer among cylindrical zones at different temperatures. Estimations can be made with them when the properties of the adsorbing media are not constant, and, as before, they are not solely applicable to cylindrical geometries.
3. From the heat transfer viewpoint alone, experimental results indicate that carbon black is an excellent seeding material for nuclear rocket use.

REFERENCES

1. Howell, J. R. and M. K. Strite, Analysis of Heat-Transfer Effects in Rocket Nozzles Operating with Very High-Temperature Hydrogen, NASA TR R-220, National Aeronautics and Space Administration, Lewis Research Center, Cleveland, Ohio, 1965.

2. Krascella, N. L., Tables of the Composition, Opacity, and Thermodynamic Properties of Hydrogen at High Temperatures, NASA SP-3005, Washington, D. C., 1963.

3. Burkig, V. C., Thermal Absorption in Seeded Gases, Douglas Report DAC-59985, Douglas Aircraft Company, Inc., Missile and Space Systems Division, Santa Monica, California, 1967.

4. Krascella, N. L., Theoretical Investigation of the Absorption and Scattering Characteristics of Small Particles, United Aircraft Corporation Research Laboratories Report C-910092-1, 1964.

5. Marteney, P. J., Experimental Investigation of the Opacity of Small Particles, United Aircraft Corporation Research Laboratories Report C-910092-2, 1964.

6. Hottel, H. C. and E. S. Cohen, "Radiant Heat Exchange in a Gas-filled Enclosure: Allowance for Non-uniformity of Gas Temperature," American Institute of Chemical Engineers, Journal 4, 3-14 (1958).

7. Erkku, H., Radiant Heat Exchange in Gas-filled Slabs and Cylinders, Ph.D. Thesis, Massachusetts Institute of Technology, 1959.

8. Hoffman, T. W. and W. H. Gauvin, "An Analysis of Spray Evaporation in a High Temperature Environment, I. Radiant Heat Transfer to Clouds of Droplets and Particles," Canadian Journal of Chemical Engineering 39, 179-88 (1961).

9. Hoffman, T. W., Theoretical and Experimental Investigation of the Evaporation of Stationary Droplets and Sprays in High Temperature Surroundings, Ph.D. Thesis, McGill University. 1959.

10. McAlister, J. A., E. Y. H. Keng and C. Orr, Jr., Heat Transfer to a Gas Containing a Cloud of Particles, Semiannual Status Report No. 6, Project A-635-002, Engineering Experiment Station, Georgia Institute of Technology, Atlanta, Georgia, 1965.

11. McAlister, J. A., E. Y. H. Keng and C. Orr, Jr., Heat Transfer to a Gas Containing a Cloud of Particles, NASA CR-325, National Aeronautics and Space Administration, Washington, D. C., 1965.

12. Eckert, E. R. G. and R. M. Drake, Jr., Heat and Mass Transfer, New York: McGraw-Hill, 1959.

13. Wiebelt, J. A., Engineering Radiation Heat Transfer, New York: Holt, Rinehart, and Winston, 1966.

14. Fishenden, M. and O. A. Saunders, "The Errors in Gas Temperature Measurements and their Calculation," Journal of The Institute of Fuel 12, No. 64, S5-S14 (March, 1939).

15. Bosanquet, C. H., "The Wall Effect in Gas Temperature Measurement," Journal of The Institute of Fuel 12, No. 64, S14-S17 (March, 1939).

16. McAdams, W. H., Heat Transmission, New York: McGraw-Hill, 1954.

17. Holl, H. B., The Reflection of Electromagnetic Radiation, Redstone Arsenal Report RF-TR-63-4, U. S. Army Missile Command, Huntsville, Ala.

18. Allen, R. D., L. F. Glassier and P. L. Jordan, "Spectral Emissivity, Total Emissivity, and Thermal Conductivity of Molybdenum, Tantanum, and Tungsten above 2300°K," Journal of Applied Physics 31, 1382-7 (1960).

19. Williams, F. A., "On the Vaporization of Mist by Radiation," International Journal of Heat and Mass Transfer 8, 575-87 (1965).

20. Friedman, M. H. and S. W. Churchill, "The Adsorption of Thermal Radiation by Fuel Droplets," Chemical Engineering Progress Symposium Series 61, No. 57, 1-4 (1965).

"The aeronautical and space activities of the United States shall be conducted so as to contribute . . . to the expansion of human knowledge of phenomena in the atmosphere and space. The Administration shall provide for the widest practicable and appropriate dissemination of information concerning its activities and the results thereof."

—NATIONAL AERONAUTICS AND SPACE ACT OF 1958

NASA SCIENTIFIC AND TECHNICAL PUBLICATIONS

TECHNICAL REPORTS: Scientific and technical information considered important, complete, and a lasting contribution to existing knowledge.

TECHNICAL NOTES: Information less broad in scope but nevertheless of importance as a contribution to existing knowledge.

TECHNICAL MEMORANDUMS: Information receiving limited distribution because of preliminary data, security classification, or other reasons.

CONTRACTOR REPORTS: Scientific and technical information generated under a NASA contract or grant and considered an important contribution to existing knowledge.

TECHNICAL TRANSLATIONS: Information published in a foreign language considered to merit NASA distribution in English.

SPECIAL PUBLICATIONS: Information derived from or of value to NASA activities. Publications include conference proceedings, monographs, data compilations, handbooks, sourcebooks, and special bibliographies.

TECHNOLOGY UTILIZATION PUBLICATIONS: Information on technology used by NASA that may be of particular interest in commercial and other non-aerospace applications. Publications include Tech Briefs, Technology Utilization Reports and Notes, and Technology Surveys.

Details on the availability of these publications may be obtained from:

SCIENTIFIC AND TECHNICAL INFORMATION DIVISION

NATIONAL AERONAUTICS AND SPACE ADMINISTRATION

Washington, D.C. 20546